2

X-750-73-263
PREPRINT

NASA TM X 70490

BIFOCAL DUAL REFLECTOR ANTENNA

B. L. J. RAO

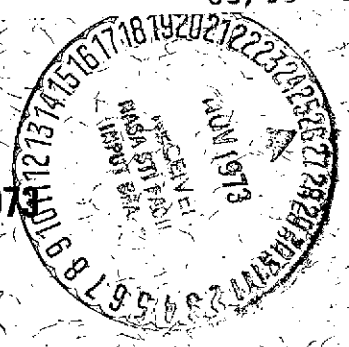

SEPTEMBER 1973

GSFC
GODDARD SPACE FLIGHT CENTER
GREENBELT, MARYLAND

X-750-73-263
Preprint

BIFOCAL DUAL REFLECTOR ANTENNA

B. L. J. Rao

September 1973

GODDARD SPACE FLIGHT CENTER
Greenbelt, Maryland

BIFOCAL DUAL REFLECTOR ANTENNA

B. L. J. Rao

Abstract — A bifocal dual reflector antenna is similar to and has better scan capability than classical cassegrain reflector antenna. The method used in determining the reflector surfaces is a modification of a design method for the dielectric bifocal lens. The three dimensional dual reflector is obtained by first designing an exact (in geometrical optics sense) two-point corrected two dimensional reflector and then rotating it around its axis of symmetry. A point by point technique is used in computing the reflector surfaces. Computed radiation characteristics of the dual reflector are compared with those of a cassegrain reflector. The results confirm that the bifocal antenna has superior performance.

CONTENTS

BIFOCAL DUAL REFLECTOR ANTENNA

INTRODUCTION

It is well known that a bifocal dielectric lens [1], [2] has a wider angle scan capability than a dielectric lens with a single focus. We propose a bifocal dual reflector antenna which has a better scan capability than a classical cassegrain reflector.

The three dimensional reflector is obtained by first designing an exact (in geometrical optics sense) two point corrected two dimensional dual reflector and then rotating it around its axis of symmetry. Figure 1 shows a cross section of a cylindrical bifocal dual reflector antenna configuration. The focal points A and B are displaced from the reflector axis of symmetry by an amount d, and the sub-reflector intersects the x-axis at x = P. The two dimensional reflector surfaces are designed so that a feed placed at A produces a beam emerging at a design scan angle α (corresponding to the phase front A), and a feed placed at B produces a beam emerging at a scan angle of $-\alpha$ (corresponding to the phase front B) as shown in Figure 1. In other words, when plane waves impinge on the reflector system at an angle α or $-\alpha$, they are focussed on to the focal points A and B respectively. However, the three dimensional reflector (obtained by rotating two dimensional reflector around its axis) does not have two perfect focal points. This is also true for a bifocal dielectric lens. The results of this study, however, show that the points A and B are still the best focal points for a three

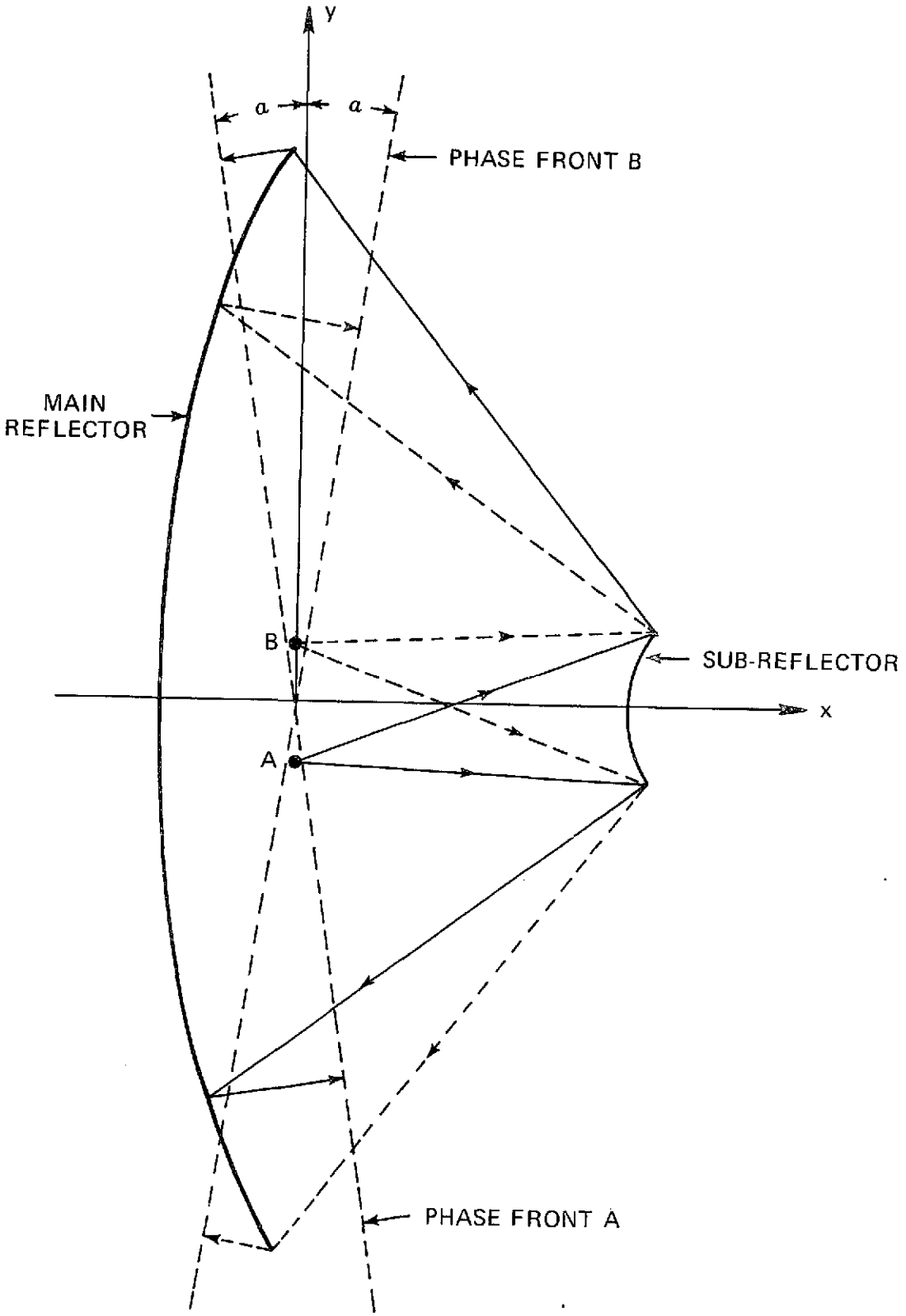

Figure 1. Two Dimensional Bifocal Dual Reflector.

dimensional bifocal reflector. A ray tracing technique will be used to determine the reflector surfaces.

Applying the ray tracing design procedure gives a series of discrete points on both the sub-reflector and the main reflector. These series of points on the reflector surfaces are then approximated by best fit (in the least squares sense) polynomials. These polynomial representations for the reflector surfaces are then used to find the radiation patterns of the proposed antenna for several scan angles using numerical methods. The computed radiation patterns are then compared with those of classical cassegrain reflector antenna. The results confirm that the bifocal reflector has a better scan capability.

DESIGN PROCEDURE

Figure 1 shows the configuration of a bifocal reflector with the y-axis of the coordinate system passes through the two foci; the origin of the coordinate system is midway between the two foci. The sub-reflector is normal to the x-axis at x = P. The design scan angle α and the path length L from each focus to its respective phasefront are assumed known. Thus we know the parameters d, P, α, L (we will discuss later how to choose these parameters in any specific design) and a single point (P, 0) (hereafter referred to as the initial point) and the slope at that point on the sub-reflector. Refer to Figure 2 for a qualitative discussion of how the ray tracing method is applied to find a series of points on the two reflectors. Ray 1 is an outgoing ray from point A passing through the initial point (x_1, y_1) on the sub-reflector and the yet unknown point (x'_1, y'_1) on

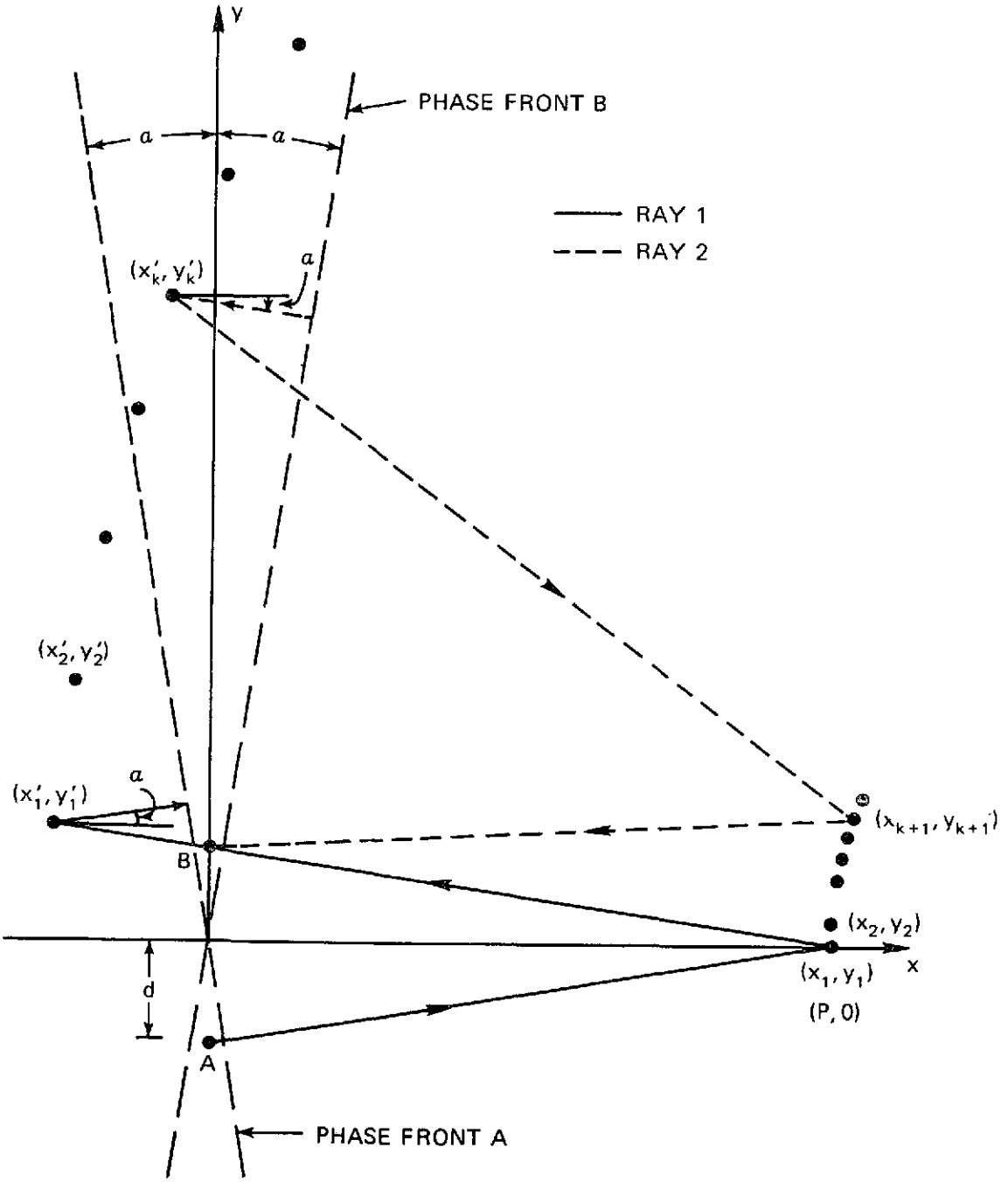

Figure 2. Raytracing Method: Initial Point is (P, 0).

the main reflector and emerging finally at an angle α to the positive x-axis. Using the parameters d, P, α, L and the initial point and the slope at that point on the sub-reflector, it is possible to find the point (x'_1, y'_1) and the slope at that point on the main reflector by applying the equal path length condition for ray 1 and Snell's law at the two reflector surfaces. The bifocal condition requires that the incoming plane wave (ray 2) incident at an angle $-\alpha$ be focussed at point B after it gets reflected at (x'_k, y'_k) and some point (x_{k+1}, y_{k+1}) on the sub-reflector. Applying the equal path length condition for ray 2, for k = 1, and Snell's law at the two reflector surfaces, it is possible to solve for the point (x_2, y_2) and the slope at that point on the sub-reflector by knowing the point (x'_1, y'_1) and the slope at that point on the main reflector. This criss-cross procedure of finding a point and a slope on the main reflector knowing a point and a slope on the sub-reflector and vice versa is continued until a predetermined main reflector diameter is reached. This procedure gives a series of points and slopes at those points on the bifocal reflector surfaces.

It should be noted that an outgoing ray is used to find a point and a slope on the main reflector when a point and a slope on the sub-reflector are known. The incoming ray is used to find a point and a slope on the sub-reflector when a point and a slope on the main reflector are known. The tracing of all outgoing rays is described by one set of formulas and the tracing of all incoming rays is described by another set of formulas. These two sets of formulas are obtained next.

Figure 3 is utilized to determine the coordinates of a point (x'_k, y'_k) and the slope on the main reflector when a point (x_k, y_k) and the slope on the sub-reflector are known. The equal path length condition for the outgoing ray shown in Figure 3 gives

$$L = R_1 + R_2 + R_3, \tag{1}$$

where

$$R_1 = \sqrt{(d + y_k)^2 + x_k^2},$$

$$R_2 = \sqrt{(x_k - x'_k)^2 + (y'_k - y_k)^2},$$

$$R_3 = -(x'_k/\cos\alpha) - (y'_k - x'_k \tan\alpha)\sin\alpha.$$

Applying Snell's law at the sub-reflector, the surface normal at (x_k, y_k) is given by (see Figures 3 and 4)

$$\left(\frac{dx}{dy}\right)_{x_k, y_k} = \tan\left(\frac{\gamma'_k - \theta'_k}{2}\right) = \tan\left(\frac{\gamma_k - \theta_k}{2}\right).$$

From this relation it is noted that γ_k is given by

$$\gamma_k = \gamma'_k - \theta'_k + \theta_k, \tag{2}$$

where $\theta_k = \tan^{-1}\left(\frac{y_k + d}{x_k}\right)$, and the values of γ'_k and θ'_k are already known from the knowledge of the slope at (x_k, y_k) and are given in (9) and (14) except for the initial values given by

$$\gamma'_1 = \theta'_1 = -\tan(d/P). \tag{3}$$

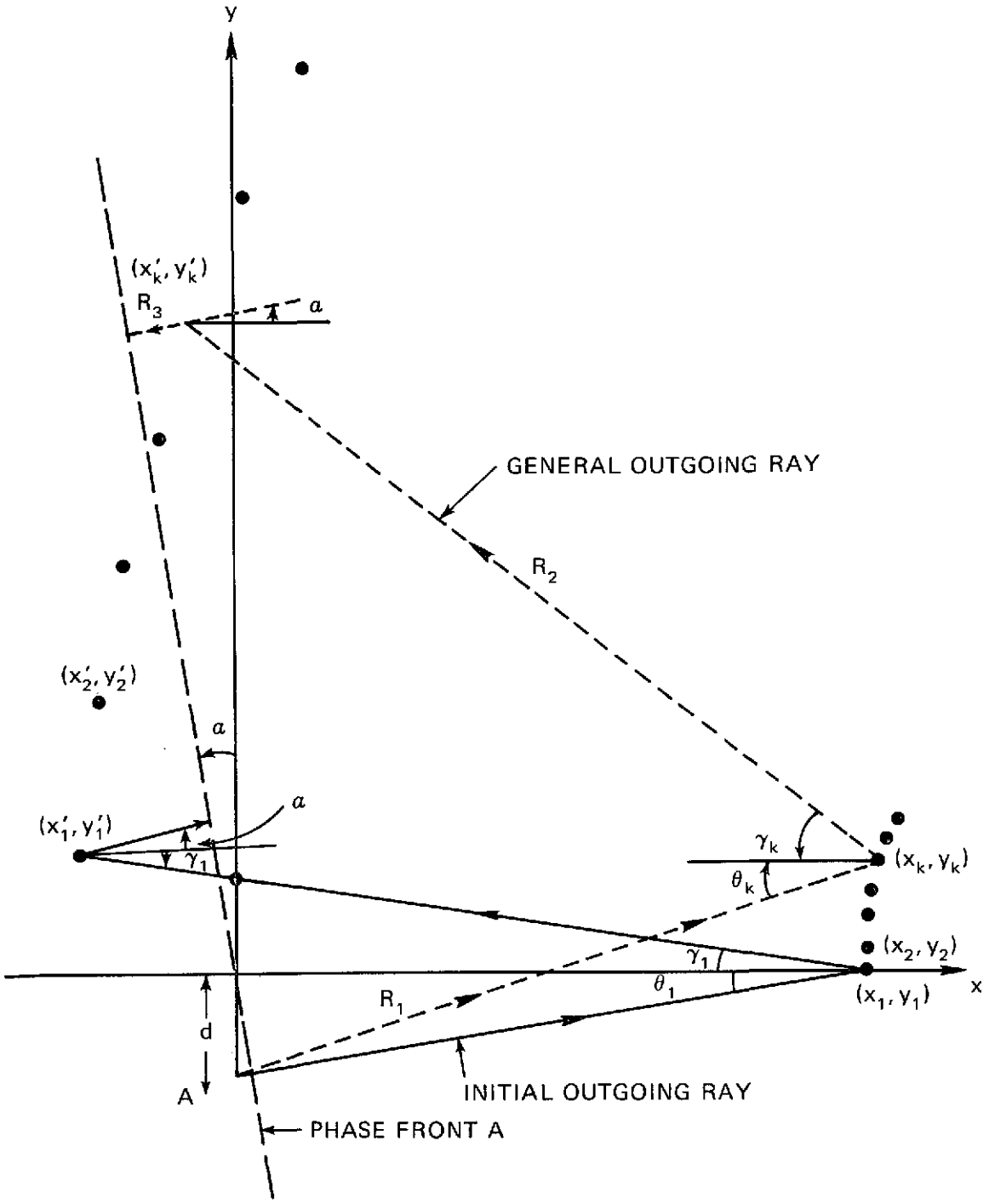

Figure 3. Finding a Point on the Main Reflector.

Having found γ_k, the following relation is obtained from Figure 3:

$$\tan \gamma_k = (y_k' - y_k)/(x_k - x_k'). \tag{4}$$

There are only two unknowns x_k' and y_k' in the two equations (1) and (4). Solving these equations gives

$$x_k' = \frac{R_1 - L + x_k w - y_k \sin \alpha}{w + \cos \alpha}, \tag{5}$$

where

$$w = \frac{1 - \sin \gamma_k \sin \alpha}{\cos \gamma_k}.$$

Once x_k' is known, equation (4) can be used to solve for y_k' as

$$y_k' = y_k + (x_k - x_k') \tan \gamma_k \tag{6}$$

The surface normal at the point (x_k', y_k') is determined from the following relation obtained from Figure 3:

$$\left(\frac{dx}{dy}\right)_{x_k', y_k'} = \tan\left(\frac{\gamma_k - \alpha}{2}\right). \tag{7}$$

Equations (2), (3), (5), (6) and (7) form the first set of formulas used to find the point (x_k', y_k') and the slope at that point on the main reflector when a point (x_k, y_k) and the slope at that point on the sub-reflector are known. For the first ray, k = 1, the initial value of γ_1' and θ_1' is given by equation (3) and the initial point (x_1, y_1) on the sub-reflector is given by (P, 0) as was noted earlier.

In a similar manner a second point (x_2, y_2) and a slope on the sub-reflector can be found knowing the point (x_1', y_1') and the slope at that point on the main reflector by tracing the incoming ray shown in Figure 4 (for k = 1). The set of formulas for the incoming rays are derived using Figure 4 and are used to find a point (x_{k+1}, y_{k+1}) and the slope at that point on the sub-reflector when a point (x_k', y_k') and the slope at that point on the main reflector are known. Applying the equal path length condition for the incoming ray shown in Figure 4 gives

$$L = R_1' + R_2' + R_3', \tag{8}$$

where

$$R_1' = \sqrt{(y_{k+1} - d)^2 + x_{k+1}^2},$$

$$R_2' = (y_k' - y_{k+1}) / \sin \gamma_{k+1}',$$

$$R_3' = -(x_k' / \cos \alpha) + (y_k' + x_k' \tan \alpha) \sin \alpha.$$

Applying Snell's law at the main reflector, the surface normal at (x_k', y_k') is given by (see equation (7) and Figure 4)

$$\left(\frac{dx}{dy}\right)_{x_k', y_k'} = \tan\left(\frac{\gamma_k - \alpha}{2}\right) = \tan\left(\frac{\gamma_{k+1}' + \alpha}{2}\right).$$

This relation gives the value of γ_{k+1}' in terms of the known values of γ_k given by equation (2) and α as

$$\gamma_{k+1}' = \gamma_k - 2\alpha. \tag{9}$$

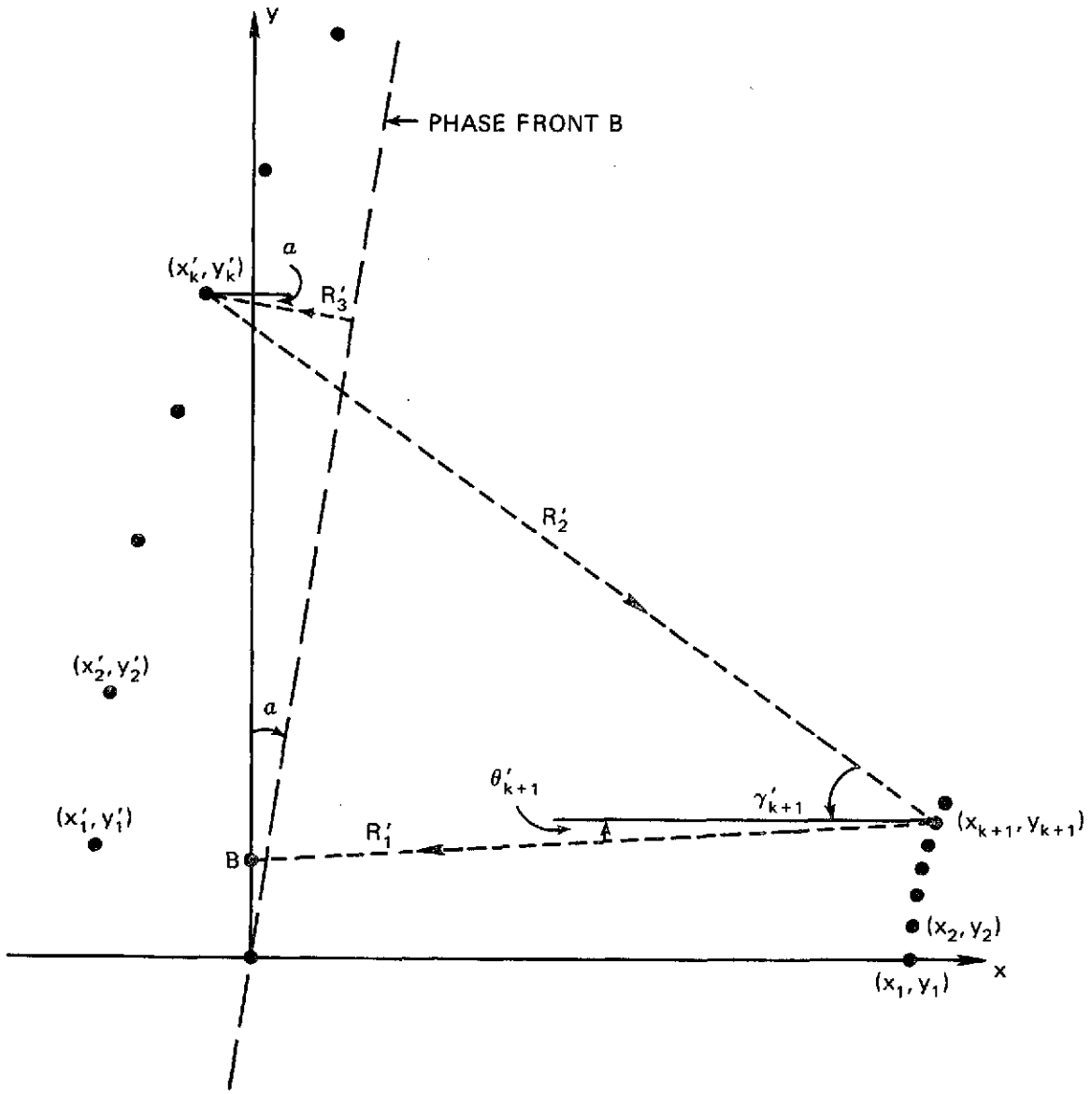

Figure 4. Finding a Point on the Sub-Reflector.

Having found γ'_{k+1}, the following relation is obtained from Figure 4:

$$\tan \gamma'_{k+1} = (y'_k - y_{k+1})/(x_{k+1} - x'_k). \tag{10}$$

There are only two unknowns x_{k+1} and y_{k+1} in the two equations (8) and (10). Solving these equations gives

$$y_{k+1} = \frac{y'_k R + .5 \sin \gamma'_{k+1} \left[d^2 + x'^2_k - (L - R_3)^2 - y'^2_k\right]}{R + (d - y'_k) \sin \gamma'_{k+1}}, \tag{11}$$

where

$$R = L - R'_3 + x'_k \cos \gamma'_{k+1}.$$

Knowing y_{k+1}, equation (10) can be used to find x_{k+1} as

$$x_{k+1} = x'_k + (y'_k - y_{k+1})/\tan \gamma'_{k+1}. \tag{12}$$

The surface normal at the point (x_{k+1}, y_{k+1}) is determined from the following relation obtained from Figure 4:

$$\left(\frac{dx}{dy}\right)_{x_{k+1}, y_{k+1}} = \tan \frac{\gamma'_{k+1} - \theta'_{k+1}}{2}, \tag{13}$$

where γ'_{k+1} is given by (9) and θ'_{k+1} is given as

$$\theta'_{k+1} = \tan^{-1}\left(\frac{y_{k+1} - d}{x_{k+1}}\right). \tag{14}$$

Equations (9) and (11) to (14) form the second set of formulas used to find a point and a slope on the sub-reflector when a point and a slope on the main reflector are known.

Starting with the initial point and its slope and making use of the first and then the second set of design formulas and continuing this criss-cross procedure, a succession of points and slopes on each reflector surface is computed. Since the reflector is symmetric, the points are reflected in the x-axis to obtain points on the reflector surfaces below the axis.

POLYNOMIAL APPROXIMATION

The design procedure discussed in the previous section gives a finite number of points and an equal number of slopes on the reflector surfaces. When specific practical examples were considered, the number of known points were too few to define the reflector surfaces adequately. In order to define the reflector surfaces completely it was necessary to use an approximation. It is convenient to approximate the reflector surfaces by best fit (in the least squares sense) polynomials. Since the reflectors are symmetrical, only even powers are required. The reflector surfaces are represented by the polynomials

$$x_S = A_1 + A_2 y_S^2 + A_3 y_S^4 + \text{-----}, \tag{15}$$

$$x_M = C_1 + C_2 y_M^2 + C_3 y_M^4 + \text{-----}, \tag{16}$$

where x_S and y_S are the sub-reflector coordinates and x_M and y_M are the main reflector coordinates.

The degree of the polynomial used to fit the data points depends on the accuracy requirements. In the example below a 4th degree polynomial was sufficient. If the number of data points available limits the degree of the polynomial, the known slopes at those points can be used to improve the accuracy.

EQUIVALENT CASSEGRAIN REFLECTOR

To compare the radiation characteristics of a bifocal reflector with that of a cassegrain reflector, it is necessary to choose equivalent reflectors. In this paper equivalence is established by making the main reflector diameters of each system and the spacing two reflectors (measured along the reflector axis) equal. The focal point for an on axis beam is the origin of the coordinate system. When specific examples are considered, the main reflector in the bifocal antenna very closely approximates a paraboloid. This means the higher order coefficients (fourth degree and above) in (16) are very small, and the equivalent parabola can be defined by the first two terms of (16) as

$$x_P = C_1 + C_2 y_P^2 \tag{17}$$

where x_P and y_P are the coordinates of the equivalent parabola. The focal length of the equivalent parabola is found from (17) and is given by

$$F = 1/4\, C_2 \tag{18}$$

From the focal length of the equivalent parabola and the other assumptions made in establishing equivalence, it can be shown that the equivalent hyperbola is defined by

$$\text{Eccentricity } e = (F + C_1)/(2A_1 - F + C_1), \tag{19}$$

$$\text{Semi-major axis } a = A_1 - (F - C_1)/2, \tag{20}$$

$$\text{Semi-minor axis } b = a\sqrt{e^2 - 1}. \tag{21}$$

The equation of the equivalent hyperbola is

$$X_H = A_1 + a\left[\sqrt{1 + (Y_H/b)^2} - 1\right], \tag{22}$$

where x_H, y_H are the coordinates of the equivalent hyperbola.

COMPARISON OF THE REFLECTOR SURFACES

For a specific example, reflector surfaces were computed for the bifocal and the equivalent cassegrain antennas, and the results are shown in Figure 5. In this example d = 1.23 ft., P = 3.28 ft., α = 4°, L = 12.3 ft. and the main reflector diameter D_M = 21.24 ft. (The procedure used to determine the parameters d, P, α, L, and D_M is given in the Appendix). This results in a sub-reflector diameter D_S = 4.1 ft. and the equivalent paraboloid focal length F = 7.61 ft. The resulting reflector surfaces are so close it is difficult to differentiate between the two antennas using the scale of Figure 5A. However, they are shown separate in Figure 5A for clarity. Figures 5B and 5C show the differences in reflector surfaces. For this example the maximum deviation in the main reflectors is .055 ft. and in the sub-reflectors it is .026 ft. These seemingly small differences in reflector surfaces make a large difference in radiation patterns.

COMPARISON OF RADIATION PATTERNS

The radiation patterns (Fig. 6) were computed using numerical integration methods developed by Schmidt [3] and an operating frequency of 4 GHz and various scan angles. Radiation patterns of an equivalent cassegrain reflector are included for comparison. From Figure 6 it can be seen that for a scanning

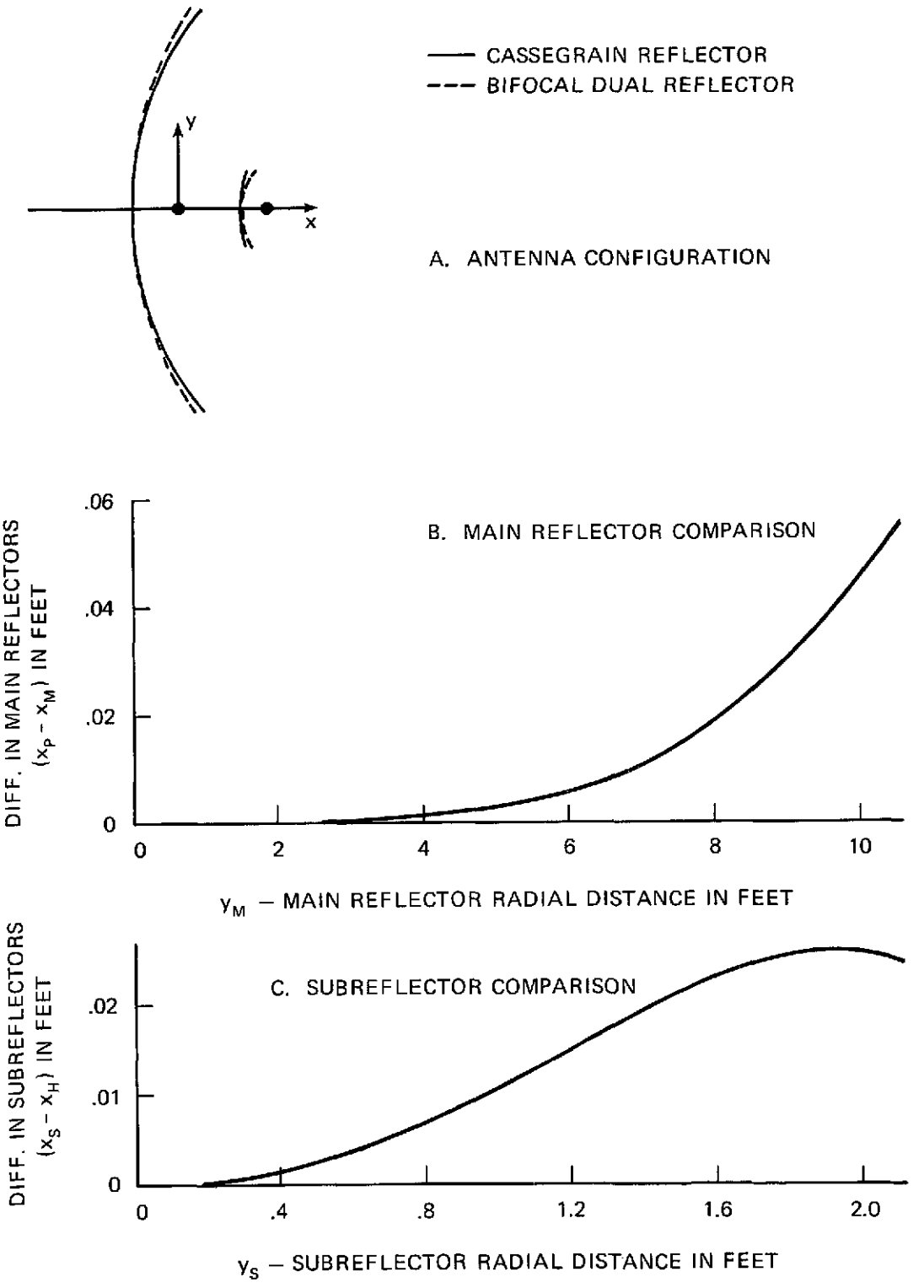

Figure 5. Reflector Surface Comparison.

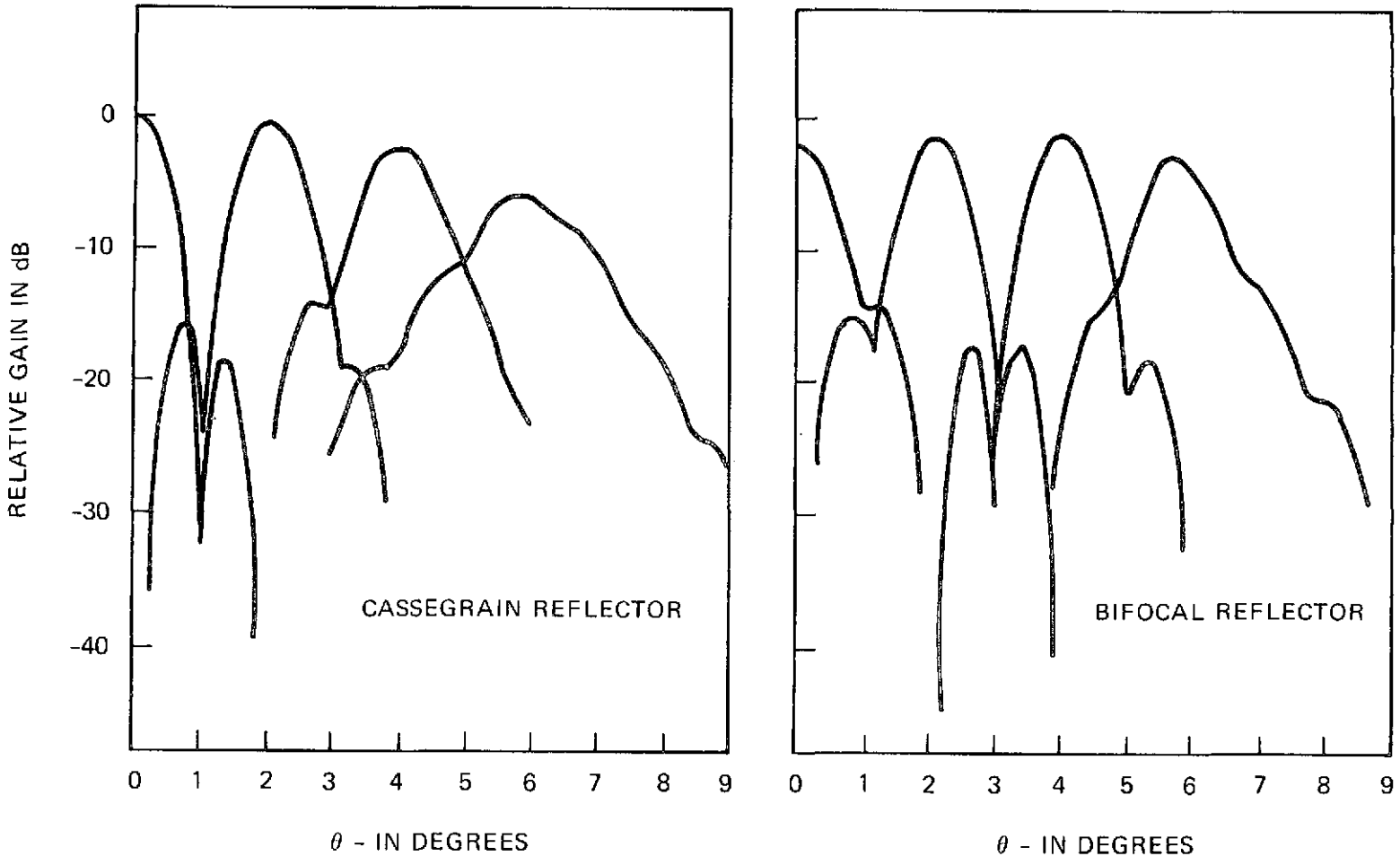

Figure 6. Radiation Patterns for Different Scan Angles (D_M = 21.24', D_S = 4.1' and Frequency = 4 GHz).

range of ±6°, the variation in gain for a bifocal antenna is only 1.5 dB as compared to 5.8 dB for the cassegrain antenna. For the same scan range, the beamwidth for the bifocal antenna varies from 0.8° to 0.9°, as opposed to 0.8° to 1.5° for the cassegrain antenna. The sidelobes are lower for the bifocal antenna except for the radiation patterns which are close to or on axis. For all the radiation patterns presented in this paper it is assumed that there is no feed amplitude taper, and the scanned radiation patterns are obtained by moving the feed along the y-axis.

Figure 7 compares the radiation patterns at 6 GHz for the same example shown in Figure 5. Again, the gain and beamwidth variations are much smaller for the bifocal antenna than the cassegrain reflector (2 dB vs. 9.3 dB and 0.6° to 0.7° vs. 0.6° to 1.2°). It is evident from Figures 6 and 7 that the bifocal antenna gives better radiation patterns when the scan angle is equal to the design scan angle (4° for the given example).

Figure 8 compares the radiation patterns when the scan angle is equal to α. As expected, the bifocal reflector gives a much better pattern (high gain, smaller beamwidth and lower sidelobes compared to a cassegrain reflector).

CONCLUSIONS

A bifocal dual reflector antenna which has a better scan capability compared to a classical cassegrain reflector is described. A design procedure for determining the reflector surfaces is discussed in detail. For a specific example, computed radiation characteristics of the bifocal reflector system are compared

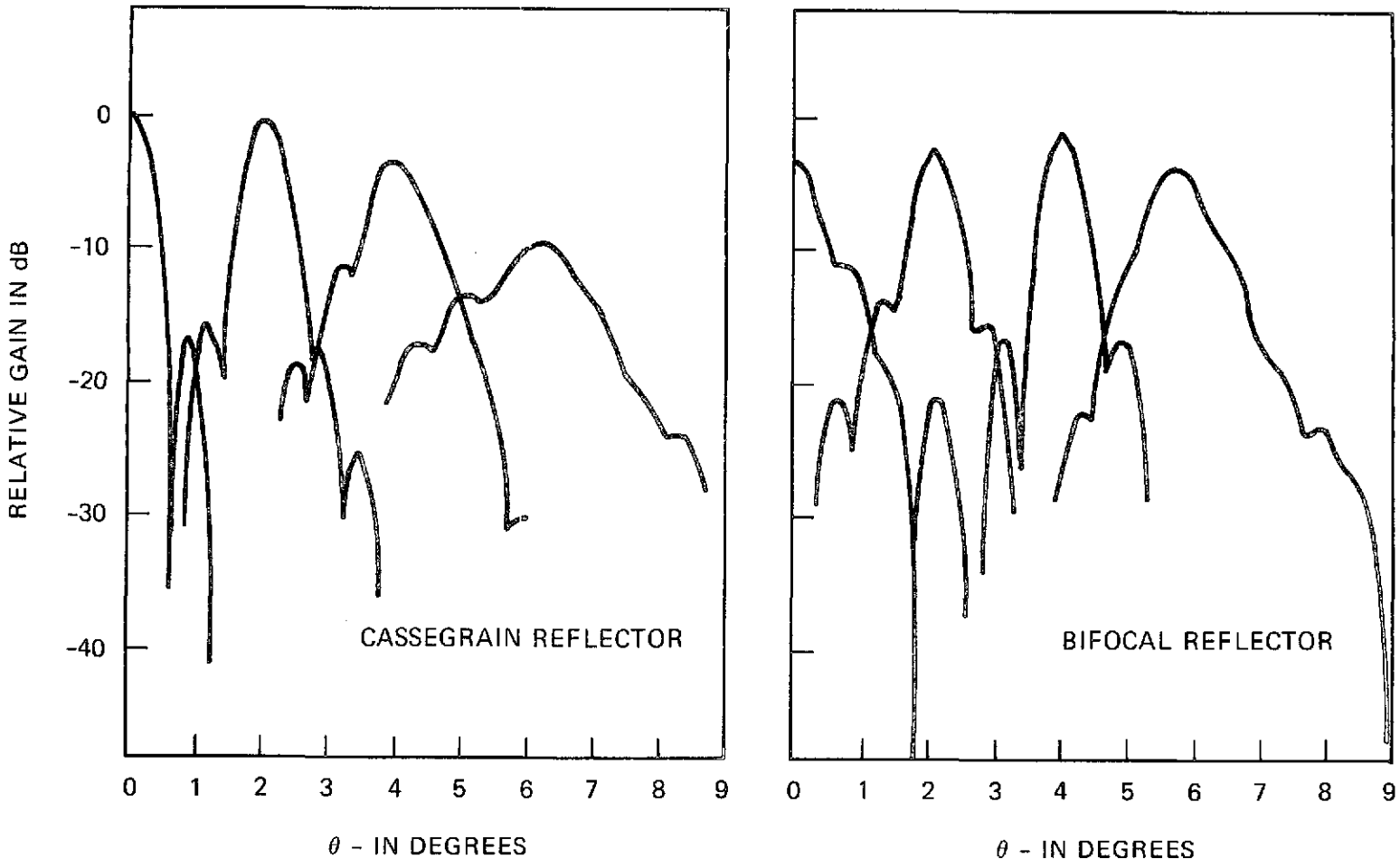

Figure 7. Radiation Patterns for Different Scan Angles (D_M = 21.24', D_S = 4.1' and Frequency = 6 GHz).

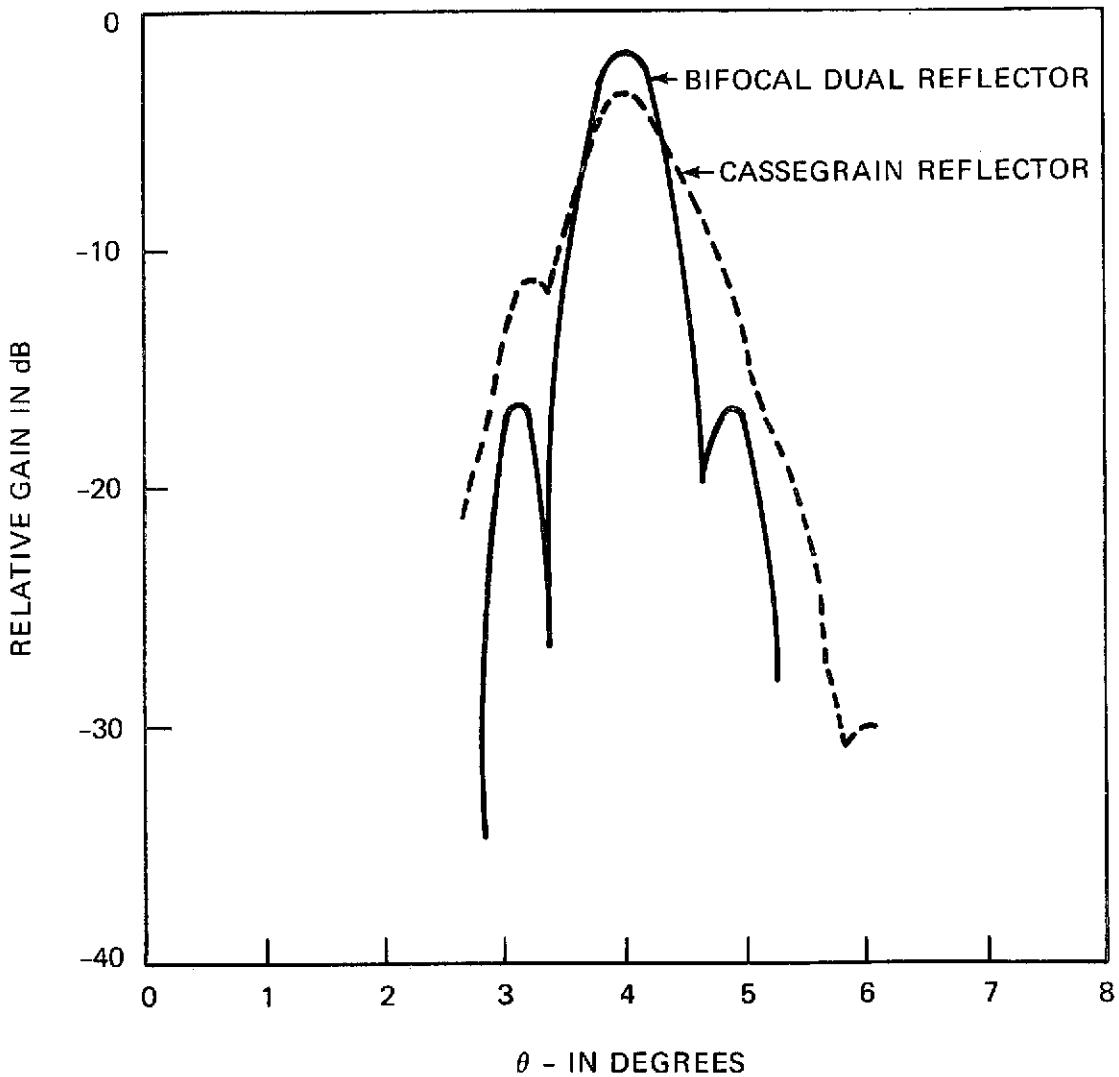

Figure 8. Comparison of Radiation Patterns at 4° Scan Angle (D_M = 21.24', D_S = 4.1' and Frequency = 6 GHz).

with those of a classical cassegrain reflector system. The results confirm that the bifocal reflector has a better scan capability. Its scanning range is sufficient to use it as a multiple beam antenna in a communications satellite. It is also very useful in applications where an off-axis gain should be more than an on axis gain.

APPENDIX

Determination of the Parameters P, L, α and d

In the design of bifocal reflector it was assumed that the above parameters are known. However, in any practical case these parameters should be chosen judiciously, otherwise the result may be unrealistic spacing between the main reflector and the sub-reflector and/or unrealistic sub-reflector diameter (may be too large or too small). Some guidelines are given here to find an initial set of parameters to satisfy certain design goals. Then, the main effect of changing these parameters is discussed so that the appropriate parameters can be changed, if needed, and a new design attempted. Since the bifocal reflector design procedure is very simple (only algebraic equations are to be solved), it is very easy to repeat the design procedure with several sets of parameters until the required spacing between the reflectors and the required sub-reflector diameter is obtained.

The design of a dual reflector antenna depends on several requirements, which can include gain, beamwidth, feed location, spacing between the reflectors and required scanning range. The gain and beamwidth depend mainly on the main reflector diameter. Therefore, the gain and beamwidth requirements do not enter the design procedure directly if all the linear dimensions are normalized to the diameter of the main reflector. The parameter P is determined from the requirement on spacing between the two reflectors. The design scan angle α is determined from the scanning requirement or the off-axis angle where the best possible pattern is required. Once α is determined, the feed displacement d is obtained from

$$d = K\alpha. \tag{A1}$$

This is similar to the relation, in the case of cassegrain reflector, between the required feed displacement d for a given scan angle α and is given by (for α small) [4].

$$d \simeq MF\alpha, \tag{A2}$$

where M is the reflector magnification and F is the focal length of the paraboloid.

Note that changing the value of K has the same effect on the bifocal reflector as changing the product MF has on the cassegrain reflector. The results of our investigation indicated that a value of K = 1 (like choosing M = 2.5 and F = .4 in the cassegrain reflector) is a good value to use in finding an initial value of d (normalized to the main reflector diameter). Note that α is in radians.

The following effects should be kept in mind when changing the initial values of the parameters P, L, α and d. If P is changed the spacing between the sub-reflector and the feed is changed. Changing L mainly affects the spacing between the two reflectors. For a given α, decreasing the value of d requires a larger sub-reflector diameter and vice versa. Similarly, for a given d, increasing α requires a larger sub-reflector diameter and vice versa.

ACKNOWLEDGMENT

The author wishes to thank Dr. E. A. Wolff for many valuable suggestions. Thanks are also due to R. F. Schmidt, R. Miezes and W. K. Bartley for developing the computer program used in obtaining the radiation patterns presented in this paper. The author also wishes to thank the National Research Council for supporting this research under the Resident Research Associateship program.

REFERENCES

[1] R. M. Brown, "Dielectric Bifocal Lenses," IRE National Convention Record, pp. 180 - 187, 1956.

[2] F. S. Holt and A. Mayer, "A Design Procedure for Dielectric Microwave Lenses of Large Aperture Ratio and Large Scanning Angle," IRE Trans. on Ant. and Prop., pp. 25 - 30, January 1957.

[3] R. F. Schmidt, "The Calculation of Electromagnetic Fields in the Fresnel and Fraunhofer Regions Using Numerical Integration Methods," NASA X-document No. X-811-71-392, Goddard Space Flight Center, Greenbelt, Maryland, June 1971.

[4] A. M. Isber, "Obtaining Beam Pointing Accuracy with Cassegrain Antennas," Microwaves, pp. 40 - 44, August 1967.